doi:10.1038/nature09765

Table S1. Genetic interactions between genes encoding muscle and CeHD proteins.

Genotype	detached muscles [1]	n
WT	4.3%	391
vab-10A(e698)	2.7%	221
egl-19(n2368)	5.7%	123
ced-10(n3246)	1,7%	117
pak-1(ok448)	3.2%	154
pix-1(gk416)	9.2%	142
git-1(tm1962)	1.6%	313
vab-10A(e698); egl-19(n2368)	89.6%	134
vab-10A(e698); ced-10(n3246)	29,3%	58
vab-10A(e698); pak-1(ok448)	62.6%	203
vab-10A(e698); pix-1(gk416)	44%	191
vab-10A(e698); git-1(tm1962)	71.1%	315
pak-1(ok448); egl-19(n2368)	16.7%	132
vab-10A(e698); egl-19(n2368);pak-1(ok448)	96,7%	212
ifb-1::GFP	9,1%	197
vab-10A(e698); ifb-1::GFP	55,5%	189

[1] Percentage of embryos with detached muscles at 15°C based on antibody staining against body wall muscles.

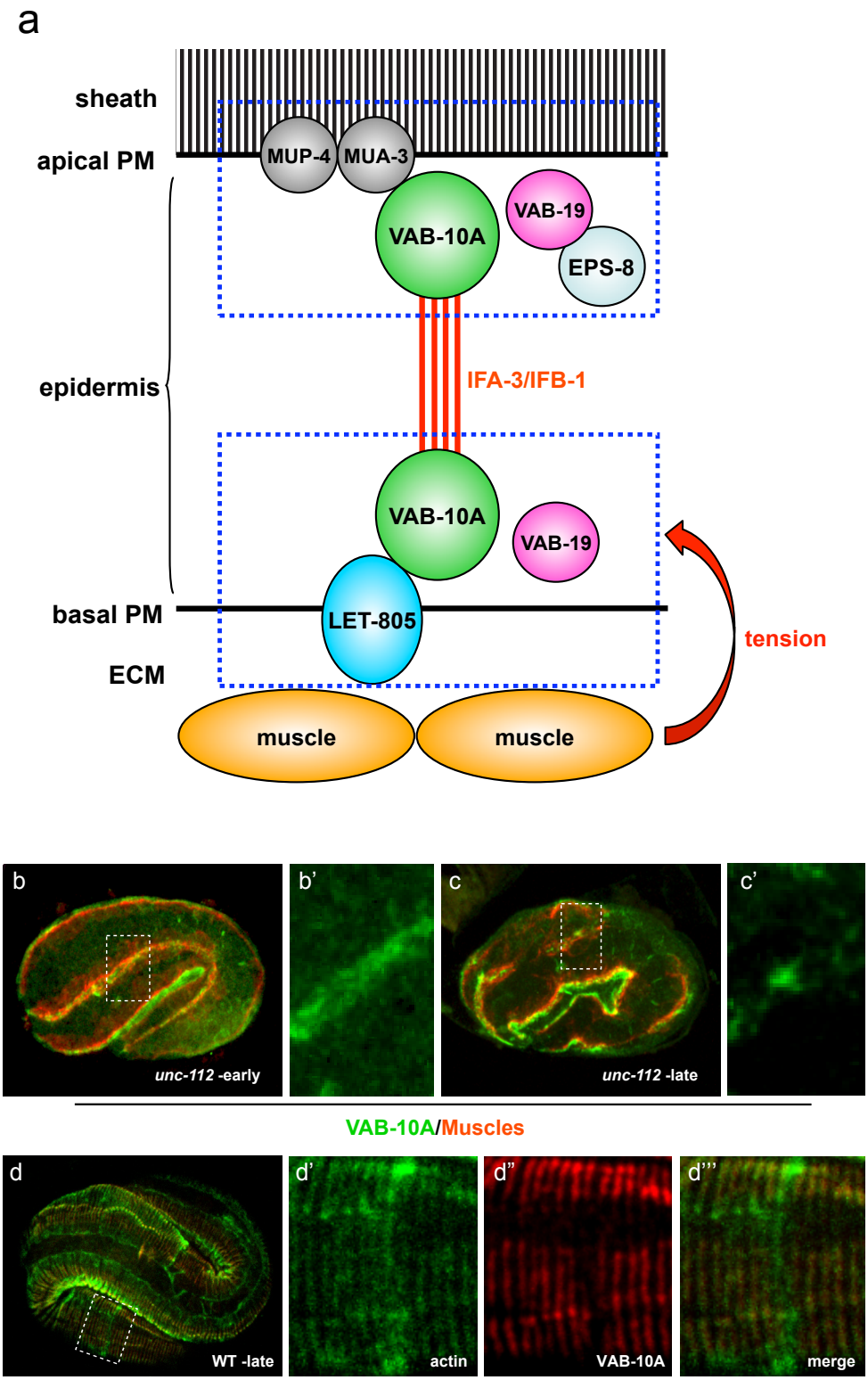
a
sheath
apical PM
MUP-4
MUA-3
VAB-10A
VAB-19
EPS-8
epidermis
IFA-3/IFB-1
VAB-10A
VAB-19
basal PM
LET-805
tension
ECM
muscle
muscle
b
b'
c
c'
unc-112 -early
unc-112 -late
VAB-10A/Muscles
d
d'
d"
d"'
WT -late
actin
VAB-10A
merge

Figure S1

Figure S1 Structure of *C. elegans* hemidesmosomes and their localization in muscle-deficient embryos

(**a**) Schematic description of a fibrous organelle (black box in Fig. 1a), made of two CeHDs (dotted blue boxes) with linking intermediate filaments (IFs) IFA-3/IFB-1. The red arrow symbolizes the mechanical input of muscles to the epidermis that goes through CeHDs. **(b-c)** Muscles (red) and VAB-10A/plakin (green) immunostaining of *unc-112(RNAi)* treated muscle-deficient embryos at early (1.5-2 fold) or late (equivalent of 3-4 fold in control embryos) stages. **(d)** VAB-10A (red) and GFP (green) immunostaining of a wild-type embryo carrying the integrated *lin-26p::ABD*$_{vab-10}$*::GFP* transgene at late stage showing colocalization of CeHD stripes and actin bundles. Scale bars, 10 µm.

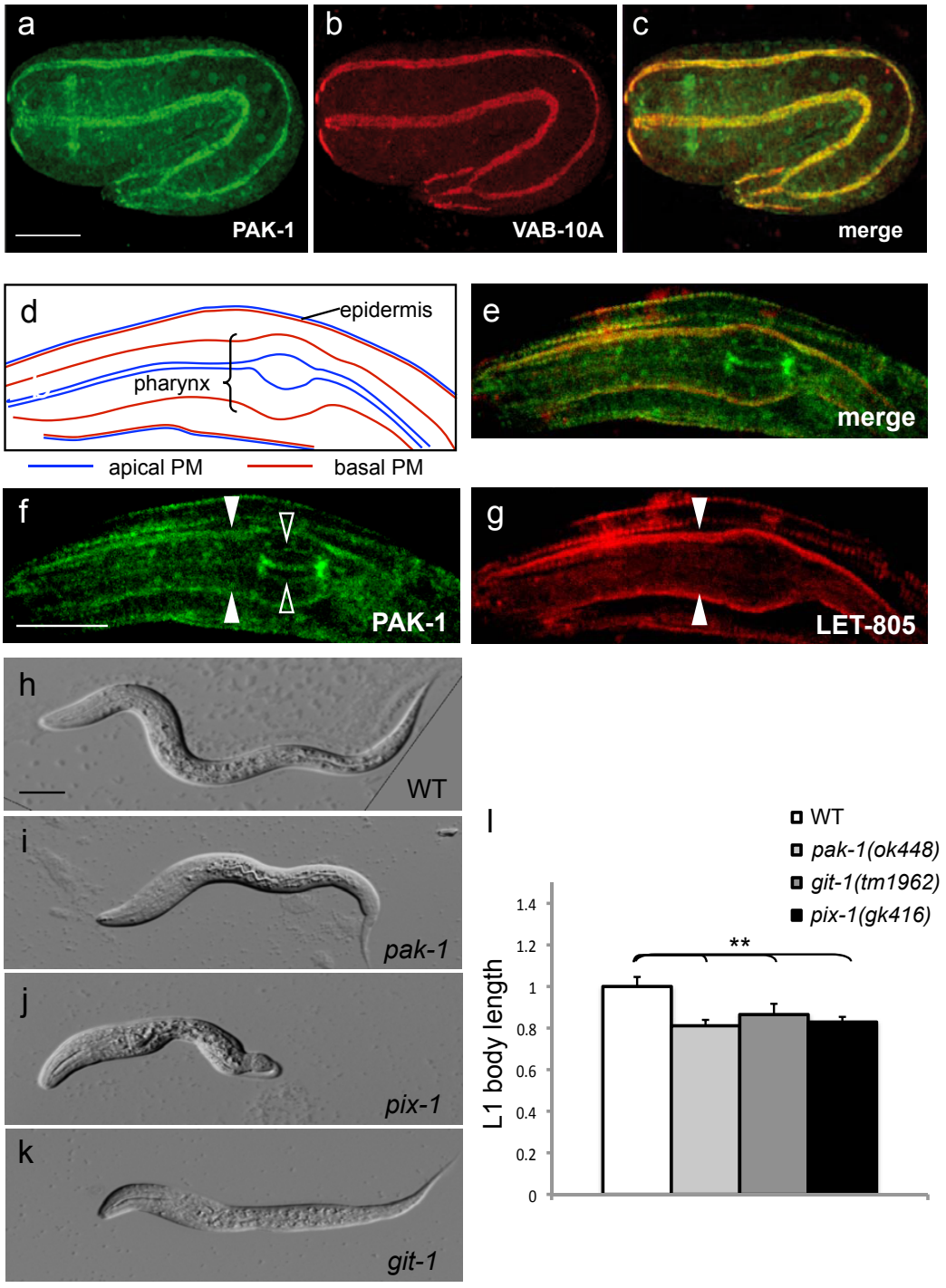
a
PAK-1
b
VAB-10A
c
merge
d
epidermis
pharynx
apical PM
basal PM
e
merge
f
PAK-1
g
LET-805
h
WT
i
pak-1
j
pix-1
k
git-1
l
WT
pak-1(ok448)
git-1(tm1962)
pix-1(gk416)
L1 body length
1.4
1.2
1
0.8
0.6
0.4
0.2
0
**

Figure S2

Figure S2 PAK-1 localization and elongation defects of PAK-1/PIX-1/GIT-1 mutants **(a-c)** Colocalization of PAK-1 and VAB-10A in an embryo at early elongation stage. **(d)** Diagram showing the *C. elegans* pharynx structure. The large pharynx epithelial cells, which anchor pharyngeal muscles, provide better apical-basal resolution than the epidermis. Pharyngeal muscles and epithelial cells are radially oriented, but not represented here in their details (for further information, see http://www.wormatlas.org/hermaphrodite/pharynx/Phaframeset.html). **(e-g)** Immunostaining with PAK-1 (green) and LET-805/myotactin (red) antibodies of the pharynx in a wild-type larva. LET-805 staining (g) marks the basement membrane (solid arrowheads) of pharyngeal epithelial cells, PAK-1 was enriched at basal CeHDs, though also present at apical CeHDs (open arrowheads in f). **(h-k)** DIC images of wild-type, *pak-1, pix-1* and *git-1* mutant L1 larvae. **(l)** Body length measurement of L1 larvae. N=24, *, p<0,00000003 Scale bars, 10 µm. Error bars, ±SEM.

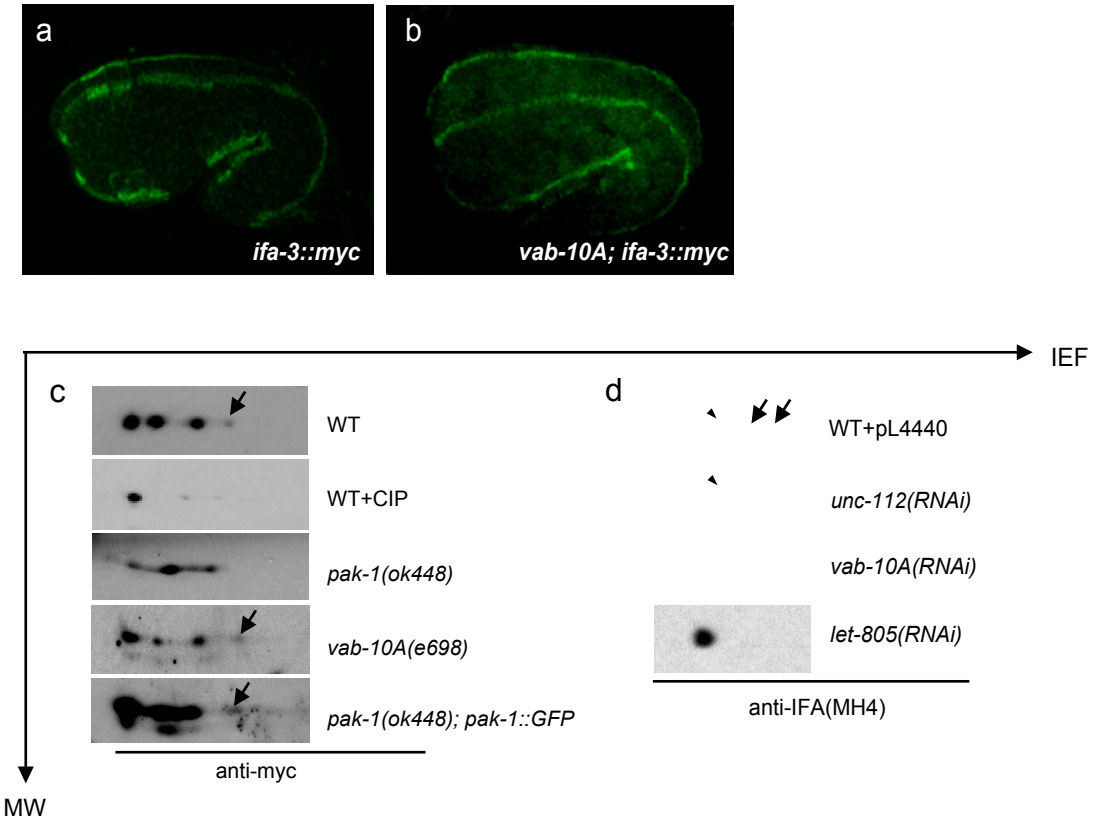
a
ifa-3::myc
b
vab-10A; ifa-3::myc
IEF
c
WT
WT+CIP
pak-1(ok448)
vab-10A(e698)
pak-1(ok448); pak-1::GFP
anti-myc
MW
d
WT+pL4440
unc-112(RNAi)
vab-10A(RNAi)
let-805(RNAi)
anti-IFA(MH4)

Figure S3

Figure S3: Intermediate filament phosphorylation and change in CeHD structure

(a-b) Expression pattern of IFA-3::MYC fusion protein in wildtype (a) and *vab-10A(e698)* (b) embryos. **(c)** 2-D immuno-transfer analysis of transgenic wild-type, *vab-10A(e698), pak-1(ok448)* embryos carrying a myc-tagged IFA-3 transgene; Western blots were probed with anti-myc M6 antibody. Phosphatase treatment indicates the existence of three phosphorylated IFA-3::myc forms (blots 1-2), one of which is missing without PAK-1 function (blot 3; see arrowhead in blot 1). *vab-10A(e698)* does not affect IFA-3 phosphorylation (blot 4). A functional PAK-1::GFP is able to rescue IFA-3::myc phosphorylation caused by loss of PAK-1 function (blot 5). **(d)** 2-D immuno-transfer analysis of embryos treated with RNAi against *unc-112* or two essential CeHD components, *vab-10* and *let-805*. Embryonic extracts were blotted with monoclonal antibodies against intermediate filaments (antibody MH4). Note that isoelectric points in wild-type extracts are missing not only from *unc-112(RNAi)* muscle-deficient embryos, but also from *vab-10A(RNAi)* or *let-805(RNAi)* treated embryos, in which CeHDs are disrupted.

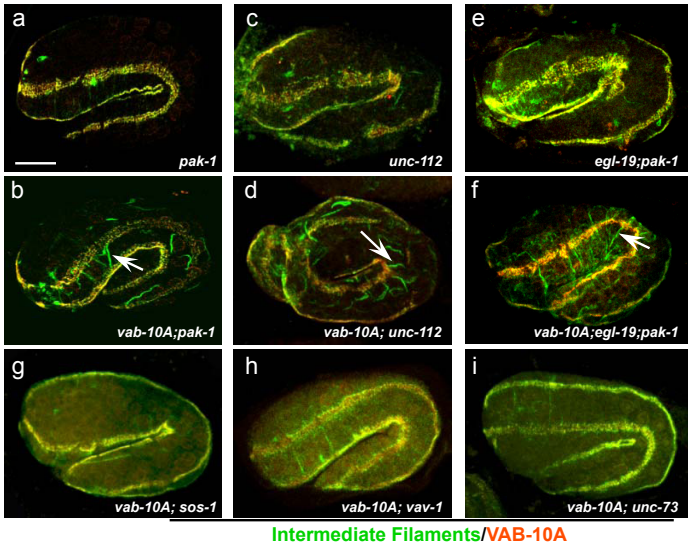
a
pak-1
c
unc-112
e
egl-19;pak-1
b
vab-10A;pak-1
d
vab-10A; unc-112
f
vab-10A;egl-19;pak-1
g
vab-10A; sos-1
h
vab-10A; vav-1
i
vab-10A; unc-73
Intermediate Filaments/VAB-10A

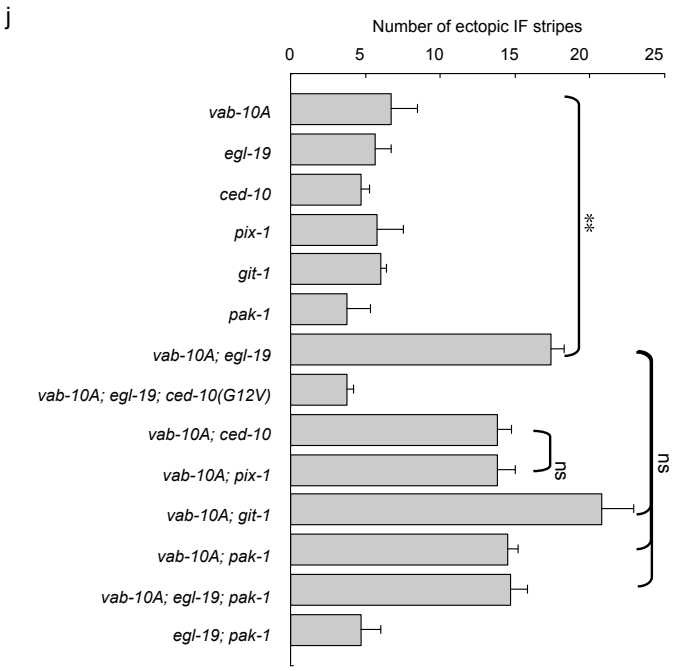
j
Number of ectopic IF stripes
0
5
10
15
20
25
vab-10A
egl-19
ced-10
pix-1
git-1
pak-1
vab-10A; egl-19
vab-10A; egl-19; ced-10(G12V)
vab-10A; ced-10
vab-10A; pix-1
vab-10A; git-1
vab-10A; pak-1
vab-10A; egl-19; pak-1
egl-19; pak-1
**
ns
ns

Figure S4

Figure S4: Intermediate filament bundling defects

(**a-h**) Immunostaining against IFs (monoclonal antibody MH4; green) and VAB-10A (polyclonal serum 4F2; red) of embryos at about the 2-fold stage with the following genotypes: *pak-1(tm403)* (a); *vab-10A(e698); pak-1(tm403)* (b); *egl-19(n2368cs); pak-1(ok448)* (e); *vab-10A(e698); egl-19(n2368cs); pak-1(ok448)* (f); control embryos after against *unc-112* (d), *sos-1* (g), *vav-1* (h) and *unc-73* (i). Embryos were kept at 15°C. **(j)** Quantification of intermediate filament ectopic bundling phenotypes in different combination of mutants involved in this study. Embryos were immuno-stained with the intermediate filament antibody MH4 and 7~15 images were taken for each genotype. The number of ectopic intermediate filament stripes in each embryo was counted by an investigator not involved in this study in a blinded fashion. Results are shown as the average number of ectopic intermediate filament stripes per embryo per genotype. Error bars, ±SEM. NS, P>0,05; **, *P*=0.000078.

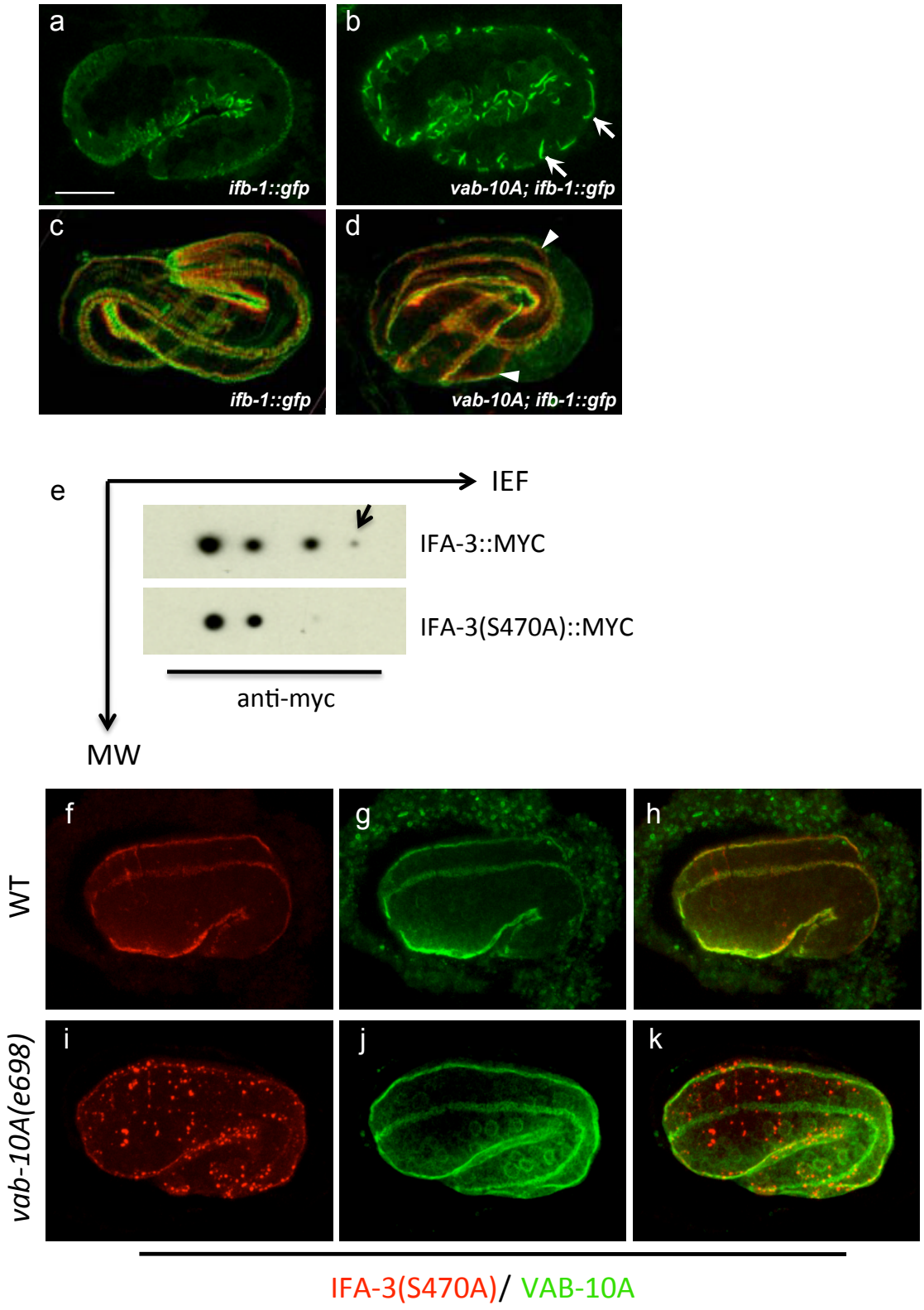
a
ifb-1::gfp
b
vab-10A; ifb-1::gfp
c
ifb-1::gfp
d
vab-10A; ifb-1::gfp
e
IEF
IFA-3::MYC
IFA-3(S470A)::MYC
anti-myc
MW
f
g
h
WT
i
j
k
vab-10A(e698)
IFA-3(S470A)/ VAB-10A

Figure S5

Figure S5: Loss of IFA-3 phosphorylation affects its CeHD localization

(a-d) Genetic interaction between *vab-10A(e698)* and an *ifb-1::gfp* transgene. Distribution of the intermediate filament IFB-1 tagged with GFP in wild-type (a) and *vab-10A(e698)* (b) embryos. Arrows point to ectopic IF stripes outside of CeHDs. Immunostaining with muscle (red) and VAB-10A (green) antibodies of wild-type (c) and *vab-10A(e698)* (d) embryos expressing an IFB-1::GFP transgene at late stages shows that muscle detached from the body wall in *vab-10A(e698)* embryos (arrowheads). **(e)** The phosphorylation profile of IFA-3(S470A)::MYC with wildtype control in embryos. Residue S470 was identified initially within a phosphorylated peptide "YQRSAKGNVsIKEVsPEGK" by a MassSpec analysis for IFA-3 (probability 56%). Software NetPhos 2.0 predicted S470 to be a highly probable phosphorylation site. 2-D gel analysis confirmed that S470A mutation results in loss of one phosphorylated form of IFA-3::MYC (arrow). **(f-k)** Immunostaining with anti-VAB-10A (green) and anti-myc (red) antibodies in transgenic embryos expressing IFA-3(S470A). Note that in the *vab-10A(e698)* background (i), the mutated IFA-3 signal at CeHD is much weaker and frequently forms cytoplasmic puncta.

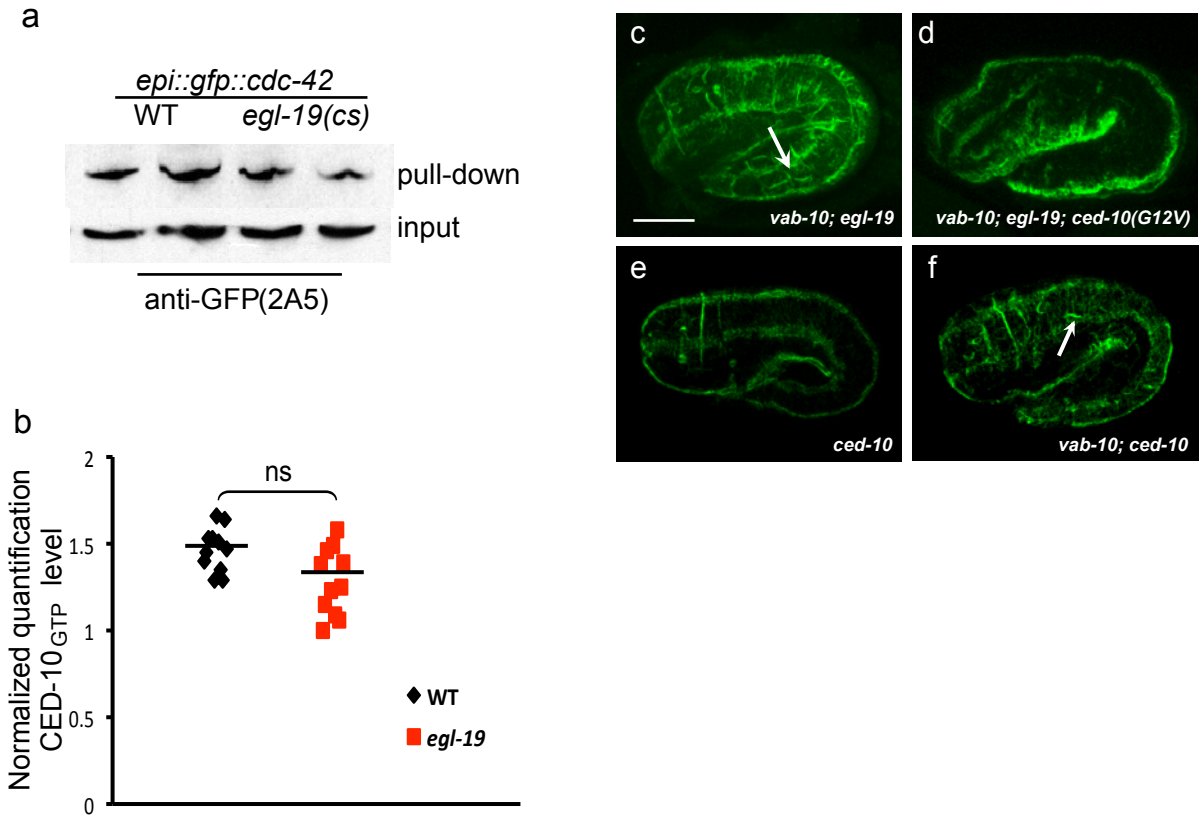

Figure S6: Muscle tension and Rac/Cdc-42 signalling

(**a-b)** Pull-down assay showing the amount of activated epidermal CDC-42 (GTP-bound form) in wild-type and muscle deficient embryonic extracts prepared from strains expressing a GFP::CDC-42 construct driven by the epidermal-specific *dpy-7* promoter (*epi::gfp::cdc-42*). (a) Total input and pull-down samples were blotted with the monoclonal antibody against GFP to specifically detect epidermal CDC-42. (b) Activated CDC-42 level was normalized by total CDC-42 in densitometry analysis. N=13, P=0.0183. **(c-f)** Immuno-staining with intermediate filaments (green) of early stage embryos kept at 15°C. Arrows, long intermediate filament bundles in *vab-10A(e698); egl-19(n2368cs)* (c), which disappeared after expression of CED-10(G12V) (d), and in *vab-10A(e698); ced-10(n3246)* (f) double mutants.

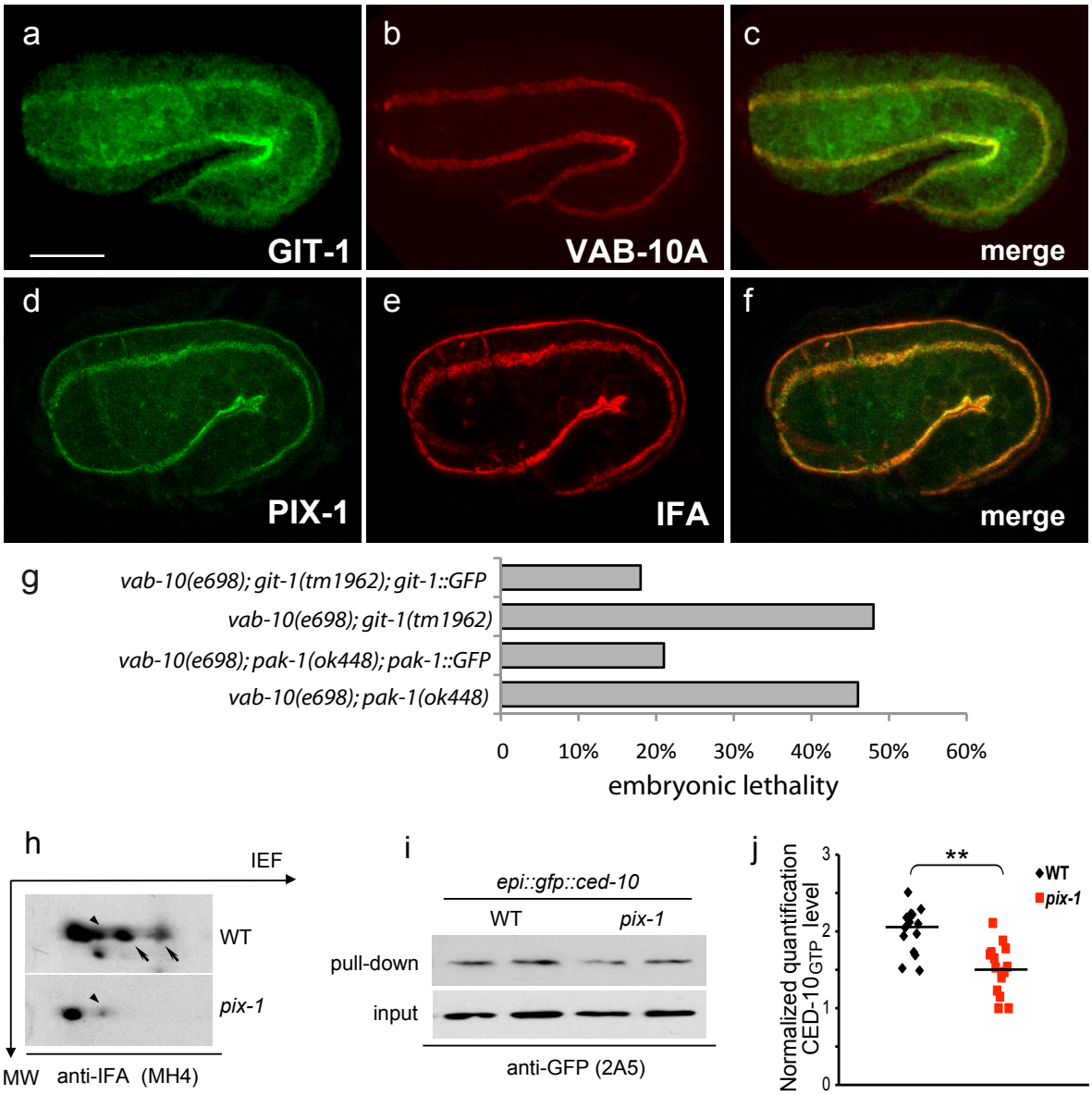

Figure S7: Distribution of translational PIX-1::GFP and GIT-1::GFP in CeHDs during elongation

(a-c) Immunostaining with GFP (green) and VAB-10A (red) antibodies of a transgenic embryo expressing a functional GIT-1::GFP construct. **(d-f)** Immunostaining with GFP (green) and IFA (red) antibodies of a transgenic embryo expressing a functional PIX-1::GFP. Both GIT-1::GFP and PIX-1::GFP colocalize with CeHD markers VAB-10A or IFA. **(g)** Embryonic lethality of *vab-10A(e698); pak-1* and *vab-10A(e698); git-1* double

mutant was partially rescued by GIT-1::GFP (70% transmission of the transgene to the progeny) and PAK-1::GFP (60% transmission of the transgene to the progeny), respectively. Given the transmission rate of each transgene, it means that most embryos with GFP fusion could be rescued, confirming that these GFP fusion proteins are functional. **(h)** 2-D analysis of wild-type and *pix-1(gk416)* embryos blotted with MH4 antibody. Arrows, isoelectric points missing in *pix-1* mutants (compare to Fig. 3b-c). **(i-j)** Pull-down assay (see Fig. 3j-k) showing the amount of epidermal-specific GTP-bound CED-10/Rac in wild-type and *pix-1(gk416)* mutant embryos (N=14). **, *P*=0.0044.

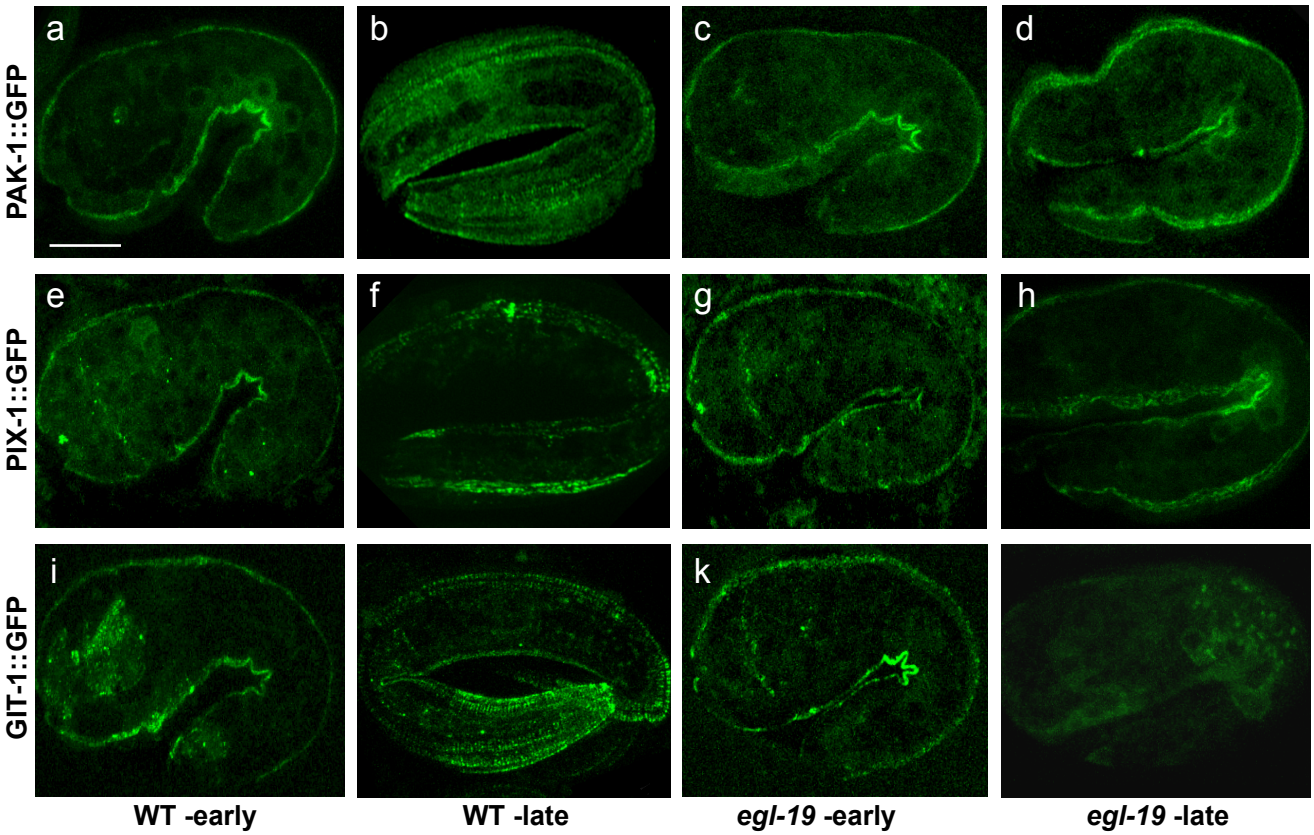

Figure S8 Muscle tension is required to maintain GIT-1, but not PIX-1 or PAK-1 localization at CeHDs.

(a-l) Representative images showing translational PAK-1::GFP (a-d), PIX-1::GFP (e-h) and GIT-1::GFP (i-l) in wild-type embryos at 1.5-fold (a,e,i) and 3-fold (b,f, j) and *egl-19(n2368cs)* mutant embryos at comparable stages (c,g.k and d,h,l). All embryos were maintained at 12°C. PAK-1 and PIX-1 still remained at hemidesmosomes after tension loss (d, h). In contrast, the localization of GIT-1 at *C. elegans* hemidesmosomes (l) was quickly lost after elongation arrest due to lack of muscle tension. Also see movie S4-7.

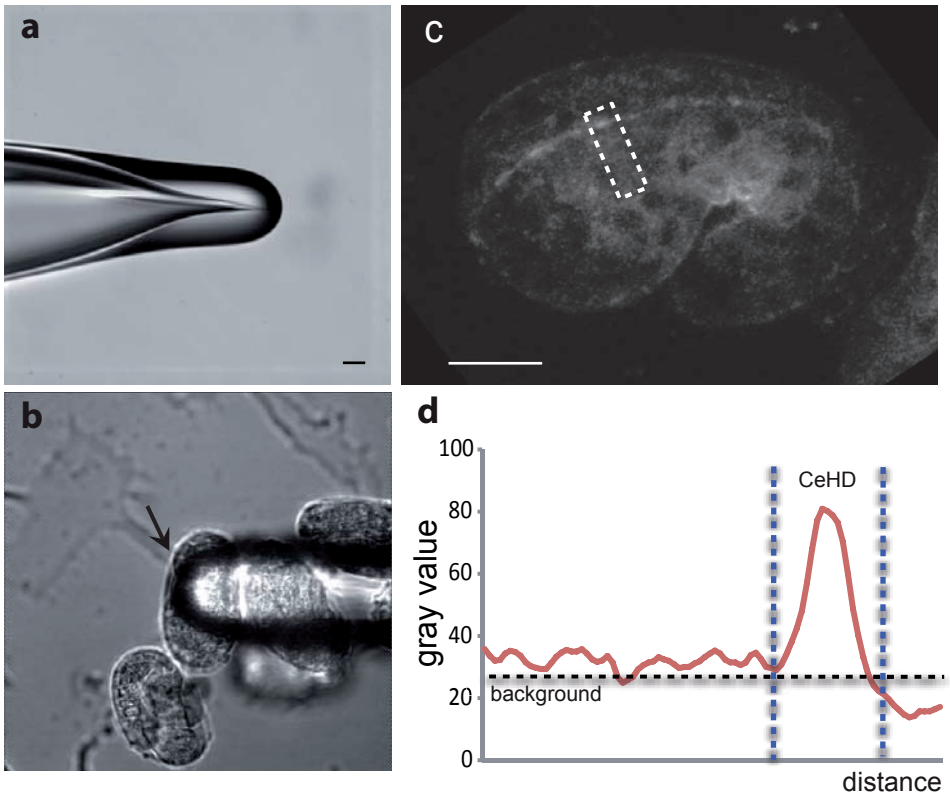

Figure S9: Montage for pressing experiments

(a) Picture of a needle used for maintaining embryos **(b)** Transmitting light image of a needle on top of an embryo (arrow). **(c-d)** Quantification of GIT-1::GFP signal at CeHDs. (d) The graph corresponds to the gray value plot profile of the selected region in (c). The GIT-1::GFP level in CeHDs is defined as the combined value within blue-lined CeHD region with the black-lined background level subtracted.

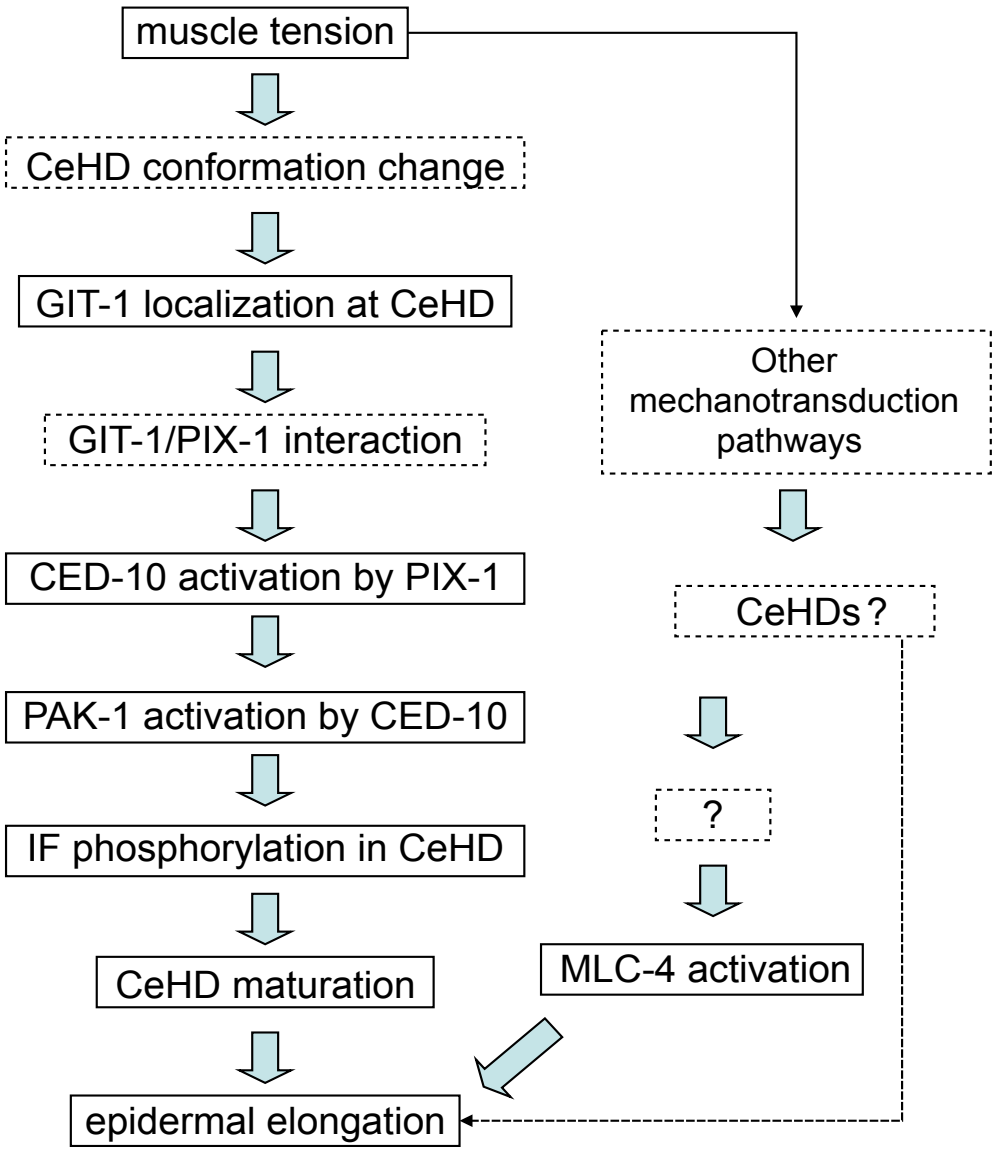
muscle tension
CeHD conformation change
GIT-1 localization at CeHD
GIT-1/PIX-1 interaction
CED-10 activation by PIX-1
PAK-1 activation by CED-10
IF phosphorylation in CeHD
CeHD maturation
epidermal elongation
Other mechanotransduction pathways
CeHDs?
?
MLC-4 activation

Figure S10

Figure S10: Schematic model of the tension-activated mechanotransduction pathway in *C. elegans* hemidesmosomes

When muscles contract they exert tension on the epidermis; we predict that this tension induces a conformational change of a CeHD component (to be defined; dotted box), which in turn helps maintain GIT-1 at CeHDs. GIT-1 presumably binds to PIX-1 (as their vertebrate counterparts do) in CeHDs and allows PIX-1 to be in a conformation state to activate Rac/CED-10. Activated Rac signalling turns on PAK-1 kinase, culminating in IFA-3 intermediate filament phosphorylation. IFA-3 phosphorylation strengthens CeHD structure, allowing embryonic elongation to continue. When muscles are inactive, GIT-1 diffuses away from *C. elegans* hemidesmosomes, and intermediate filaments are not phosphorylated, which makes the hemidesmosome weaker. When combined with *vab-10A(e698)* mutation, the de-phosphorylated IFs display ectopic bundles. We postulate the existence of other mechano-sensitive pathways triggered by muscle tension that contribute to promoting epidermal cell shape changes during embryonic morphogenesis. One of them presumably triggers myosin II activation through a pathway to be identified, which might also involve CeHDs. Solid boxes, results shown in this study. Dotted boxes, untested predictions.

Supplementary Movie Legends

Movie S1-3 Tension change in *C. elegans* epidermis triggered by muscle contraction Contracting wild-type (1), paralyzed *unc-112(RNAi)* (2) or *vab-10(RNAi)* (3) early stage embryos carrying an actin-binding GFP reporter visualizing actin bundles. Frames were recorded every 50 ms and movies were replayed with 3 frames per second.

Movie S4-7 Muscle tension is required for GIT-1, but not PAK-1 localization in CeHDs Wild-type (4, 6) or paralyzed *unc-112(RNAi)* treated (5, 7) early stage embryos carrying translational PAK-1::GFP (4, 5) or GIT-1::GFP reporter (6, 7). Frames were recorded every 5 minutes and movies were replayed with 3 frames per second. Note that over the 90 minutes of the movie, control embryos elongate significantly from the early 1.7-fold stage to almost the late 3-fold stage.